PROCEEDINGS OF ECOS 2022 - THE 35TH INTERNATIONAL CONFERENCE ON
EFFICIENCY, **C**OST, **O**PTIMIZATION, **S**IMULATION AND ENVIRONMENTAL IMPACT OF ENERGY SYSTEMS
3-7 JULY, 2022, COPENHAGEN, DENMARK

Energy and Exergy Assessment of Renewable Energy Storage using Iron as Energy Carrier

Jannik Neumann[a], Elisa Corbean[b], Frank Dammel[a], Stefan Ulbrich[b], Peter Stephan[a]

[a] Institute for Technical Thermodynamics, Technical University of Darmstadt, Darmstadt, Germany, neumann@ttd.tu-darmstadt.de
[b] Department of Mathematics, Technical University of Darmstadt, Darmstadt, Germany, corbean@mathematik.tu-darmstadt.de

Abstract:
The transformation to a climate-neutral electricity economy makes the sustainable generation of electricity from renewable energies a key technology. However, the widespread use of renewable energy faces several challenges, especially its volatility and locally limited availability. Addressing the temporal and geographic mismatch between renewable energy supply and demand is therefore crucial for a successful carbon-neutral electricity economy. Large-scale, transportable, and storable energy carriers are a key element in redressing this imbalance. Besides hydrogen-based fuels, metal fuels and iron in particular are promising alternatives to serve this purpose: electrical energy from renewable sources is stored by thermochemical reduction of iron oxides with green hydrogen and can be converted back into electricity by thermochemical oxidation (e.g., in retrofitted coal-fired power plants) spatially and temporally separated from the storage process. Despite the increasing interest in metal fuels, not many cycle analyses are available. This study provides quantitative and qualitative information on the thermodynamic performance of two thermodynamically controlled regeneration processes for iron oxides utilising a shaft furnace and a flash reactor, respectively. For the shaft furnace direct reduction of iron oxides energetic and exergetic efficiencies of 59.4 % and 51.4 %, respectively, are determined. A sensitivity analysis indicates that energetic efficiencies up to 63.0 % might be achievable within the model assumptions. The evaluation of the flash reactor direct reduction of iron oxides shows energetic and exergetic efficiencies of 68.5 % and 59.9 %, respectively. In this case, optimal values based on sensitivity analyses lead to an energetic efficiency of 71.0 % within the model assumptions. In addition to the use of commercial software, a modelling environment with direct access to mathematical optimisation techniques is in development and showcased for the flash reduction process leading to energetic efficiencies of 73.1 %. The developed models are the foundation for future thermoeconomic evaluations.

Keywords:
Recyclable Metal Fuels; Thermochemical Reduction of Iron Oxides; Shaft Furnace direct Reduction; Flash Reactor direct Reduction.

1. Introduction

Energy-related emissions were responsible for 76.2 % of all global greenhouse gas emissions in 2018 [1]. It is widely recognized that the intensified use of Renewable Energy (RE) sources in combination with increasing electrification in all sectors plays a decisive role to achieve the 1.5 °C target. This is reflected in global expansion strategies for the use of REs. However, RE sources have two major drawbacks: temporal intermittency and their uneven local availability. Electricity generation from wind power and photovoltaic plants is subject to fluctuations that lead to a temporal mismatch between availability and demand. Short-term fluctuations (hours - days) from domestic wind power and photovoltaic plants can be balanced in perspective with technologies such as pumped storage power plants or batteries. Long-term fluctuations (seasons - years), on the other hand, pose a more profound challenge. Despite ambitious RE expansion strategies, the increasing electricity demand in countries with low potential for RE (including geographic, sociological, and technological constraints) may not be met by domestic RE sources, as for example in Germany. Even though the share of REs in gross final electricity consumption is increasing (from 6.3 % in 2000 to 45.3 % in 2020 [2]), Germany is heavily dependent on energy imports (i.e., 77 % of its total primary energy supply in 2020 was covered by imports [3]), which makes self-sufficient supply with domestic renewables a major challenge due to the required electrification combined with limited RE potentials.

A promising solution for both aspects (imbalance between demand and availability, limited self-sufficient supply) is the use of carbon-neutral energy carriers. These can be synthesised with RE sources in regions with high RE potential and transported to regions with low RE potential, where they can be stockpiled and used like today's conventional fossil fuels to generate electricity on demand. Such energy carriers should be easily

transportable and storable over long time periods, enabling the global trade of renewable energy as commodity.

Currently, the most widely considered energy carrier for REs is hydrogen. However, hydrogen has a low volumetric energy density even at high pressure or in liquefied form (see Fig. 1), which makes efficient transport and storage difficult due to energy losses during liquefaction (20 % up to 40 % of the energy content based on the Lower Heating Value (LHV) of hydrogen [4]) or compression (13 % of the energy content at 70 MPa based on the LHV of hydrogen [5]).

At the same time, metal fuels have recently gained attention as candidates for recyclable energy carriers [6–8]. Metal powders can be used to fuel power-generation applications by burning them with ambient air producing metal oxides and heat or by the metal–water reaction which produces solid metal oxides, heat and hydrogen. The resulting metal oxides can be collected and regenerated with renewable energy sources, leading to a circular economy, which is depicted in Fig. 2. Due to their high volumetric energy density, the possibility of recycling them with the help of renewable energy, transporting and storing them without losses when protected from moisture and the ambient atmosphere, metal fuels are considered the most promising carbon-free energy carriers [6]. Metal fuels with a high potential are aluminium and iron due to their high volumetric energy density (cf. Fig. 1), abundance, recyclability through renewable energy, and non-toxicity. While iron might be more suitable for direct combustion with air, since theoretically no nanoparticles are created during combustion, allowing efficient collection for recycling [7], aluminium shows high reactivity with water allowing to produce heat and hydrogen on demand [9]. However, handling fine aluminium powder poses dangers, as it forms explosive mixtures with air. Both metals are promising globally tradable renewable energy carriers and are currently subject of research. This work focuses on iron as recyclable metal fuel and especially its thermochemical regeneration utilising green hydrogen.

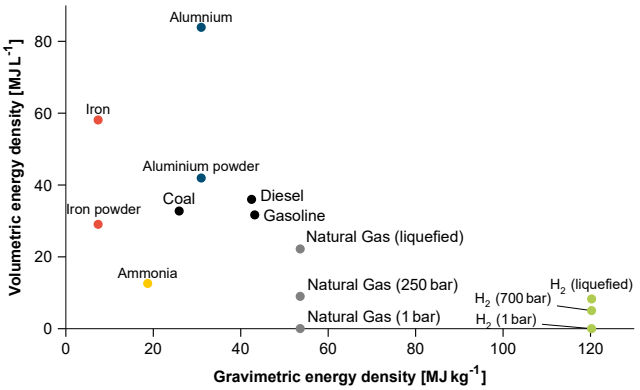

Figure 1: Energy densities of selected energy carriers. Adapted from [10].

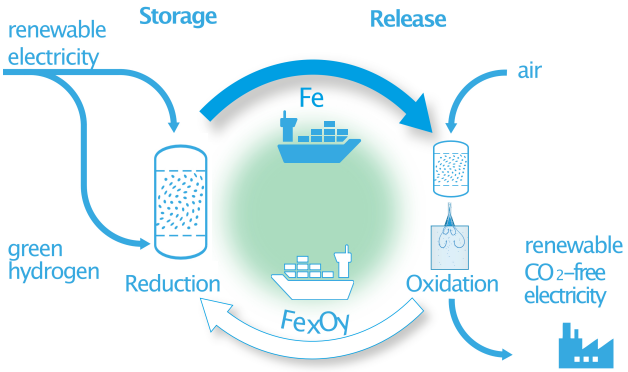

Figure 2: Energy-iron cycle [11].

Dispersions of iron particles with particle sizes of approximately 20 µm show combusting velocities comparable to those of hydrocarbon fuels, suggesting that metal fuels can be oxidised in similar burners. Existing burners could possibly be retrofitted, taking into account fuel dispersion, combustion stabilisation, and solid metal oxide product capture [7]. As proof of concept, a 100 kW iron combustor was successfully operated in the Netherlands (Technology Readiness Level (TRL) 4-5), while a follow up, the demonstration of a 1 MW combustor, is currently planned (TRL 6) [12]. These recent progresses illustrate, that iron powders could be used in existing retro-fitted coal power plants. This allows the usage of existing infrastructure, which will be redundant in the near future, to cover the increasing demands in sustainable power generation. Therefore, significantly reducing the time required for implementation and the associated investment costs.

For the thermochemical regeneration of iron oxides, available and perspective technologies from the iron and steel industry can be utilised. To date, the most common way of iron/steel production is by the use of blast furnace processes. In these processes, coke and other fossil fuels serve as reducing agents and heat sources. As an alternative to the blast furnace process, direct reduction of iron with reducing gases (H_2 + CO), usually produced by reforming natural gas, can be used in shaft furnaces. In these processes, 100 % hydrogen can be used as a reducing agent, which enables the carbon neutral reduction of iron oxides using green hydrogen. As an alternative to the shaft furnace process, a relatively new process based on a flash reactor, in which pure hydrogen can also be used as a reducing agent, can further reduce energy requirements. Both processes are promising alternatives to regenerate oxidised iron particles with green hydrogen. In the following, both processes are described, modelled, and evaluated with respect to their thermodynamic efficiencies.

2. Modelling and Evaluation

The centre of the later introduced processes is the thermochemical reduction reaction between hydrogen and iron oxides, which is briefly described in the subsequent section. To evaluate the processes, energy and exergy analyses are carried out using commercially available software. Parallel to the use of commercial software, a modelling environment with direct access to mathematical optimisation techniques is currently being developed and is presented shortly.

2.1. Reduction of Iron Oxides with Hydrogen

The stepwise direct reduction of iron oxides with hydrogen at temperatures above 843 K proceeds from hematite (Fe_2O_3) via magnetite (Fe_3O_4) to wüstite (FeO) and finally to metallic iron (Fe) [13]. Unlike the reduction of iron oxides using carbon-based reducing agents, the overall reduction of hematite with hydrogen to iron and water is endothermic

$$Fe_2O_3 + 3\,H_2 \longleftrightarrow 2\,Fe + 3\,H_2O \qquad \Delta H_r = 98.77\,\mathrm{J\,mol^{-1}}. \tag{R1}$$

The reduction is modelled on the basis of chemical equilibrium calculations [14]. The two decisive parameters for the chemical equilibrium are the reactor temperature T_R and the available hydrogen, which is quantified in the hydrogen equivalence ratio λ_{H_2}.

$$\lambda_{H_2} = \frac{\text{available hydrogen quantity}}{\text{stoichiometric required hydrogen quantity}} \quad \left[\frac{\text{mol}}{\text{mol}}\right] \tag{1}$$

Increasing both factors shifts the equilibrium to the desired side of the reaction due to Chatelier's principles.

2.2. Energetic Analysis

Since chemical reactions are involved, the physical enthalpy h_{ph} (change in enthalpy due to change in state variables), is supplemented by the chemical enthalpy h_{ch} leading to the total enthalpy h_{tot} (not to be confused with the stagnation enthalpy). The unconventional nomenclature is in accordance with the conventional nomenclature for exergy which is later introduced (see Section 2.3.).

$$h_{tot} = h_{ph} + h_{ch} \tag{2}$$

For an open control volume with a potential chemical reaction, in- and outgoing mass flow rates $\dot{m}$, the time rate of energy transfer associated with heat $\dot{Q}$ and the time rate of energy transfer associated with work (power) P, the steady state energy balance can be written as follows

$$\dot{Q} + P = \sum_{in,i} \dot{m}_i h_{i,tot} - \sum_{out,j} \dot{m}_j h_{j,tot}. \tag{3}$$

The chemical enthalpy $h_{ch,k}$ of species k is equal to the (Higher) Heating Value ((H)HV) and corresponds to $7380\,\mathrm{kJ\,kg^{-1}}$ and $141\,289\,\mathrm{kJ\,kg^{-1}}$ for iron and hydrogen, respectively.

For a reduction process with an ingoing hematite mass flow (h_{tot,Fe_2O_3}=0), electrical power supply for the subprocess and an outgoing mass flow rate of iron, the energetic system efficiency η_{sys} is given by (4). The gain of the process is the time rate of chemical energy stored in the iron stream ($\dot{m}_{Fe} \cdot h_{ch,Fe}$) and the effort is equal to the sum of the supplied powers ($\sum_i P_i$).

$$\eta_{sys} = \frac{\dot{m}_{Fe} \cdot h_{ch,Fe}}{\sum_i P_i} \tag{4}$$

2.3. Exergetic Analysis

The previous introduced nomenclature (physical, chemical, total enthalpy) is in accordance with the conventional nomenclature for exergy. In the same manner, the total specific exergy e_{tot} associated with a stream of matter can be divided into physical e_{ph} and chemical exergy e_{ch} [15],

$$e_{tot} = e_{ph} + e_{ch}. \tag{5}$$

While physical exergy is based on the (physical) enthalpy h and entropy s at the current and the reference state (subscript 0)

$$e_{ph} = (h - h_0) + T(s - s_0), \tag{6}$$

chemical exergy consists of a reactive part (standard chemical exergies) and a non reactive part due to mixing

$$e_{ch} = \sum_k x_k e^0_{ch,k} + T_0 \sum_k R_k y_k ln(y_k). \tag{7}$$

The standard chemical exergy $e^0_{\mathrm{ch},k}$ for species k can be taken from tables for standard reference environments or must be determined for a process-dependent reference environment. Here, the latter is used, where the reference species are liquid H_2O, Fe_2O_3 and ambient air. The variables x_k, y_k and R_k in (7) correspond to the mass fraction, mole fraction and the specific gas constant of species k, respectively. The calculation of standard chemical exergies for non reference species can be found in [15]. For iron and hydrogen the standard chemical exergies based on the process-dependent thermodynamic reference environment are 6448 kJ kg^{-1} and 118 246 kJ kg^{-1}, respectively.

The steady-state exergy balance with in- and outgoing mass flow rates, heat supply, and power supply is

$$\dot{E}_\mathrm{D} = P + \dot{E}_\mathrm{Q} + \sum_{in,i} \dot{m}_i e_{i,\mathrm{tot}} - \sum_{out,j} \dot{m}_j e_{j,\mathrm{tot}} - \dot{E}_\mathrm{L}, \tag{8}$$

where $\dot{E}_\mathrm{Q}$ and P correspond to the time rates of exergy transfer associated to heat and work transfer, respectively. The time rates of exergy losses $\dot{E}_L$ and exergy destruction $\dot{E}_\mathrm{D}$ depend on the specified system boundary. By varying the system boundaries, losses and destruction can change, but the absolute value for the sum remains constant. In this evaluation, all system boundaries extend into the environment with the constant reference temperature T_0. As a result, all exergy reductions due to heat losses to the environment are accumulated in the exergy destruction.

The exergetic efficiencies are defined in the same manner as the energetic efficiencies (4) by replacing the enthalpy with the corresponding exergy,

$$\epsilon_\mathrm{sys} = \frac{\dot{m}_\mathrm{Fe} \cdot e_\mathrm{ch,Fe}}{\sum_i P_i}. \tag{9}$$

All simulations are performed using the process simulation software EBSILON® Professional [16] with the included thermodynamic libraries using NASA polynomials [17]. The exergy reference temperature is set to $T_0 = 298.15$ K, and the reference pressure to $p_0 = 101.3$ kPa.

2.4. Framework for Mathematical Optimisation

In addition to the simulations using commercially available software and the energy and exergy analyses based thereon, a process simulation framework for process modelling and direct optimisation is being developed. This allows to overcome conventional iterative design methods applying heuristics and engineering judgement to individual decision variables (e.g., process variables, topology options, equipment selection) leading to non-optimal design and operation of processes. Due to the direct accessibility of advanced mathematical optimisation techniques, the iterative optimisation procedure can be replaced by advanced optimisation algorithms leading to global optimal solutions with respect to the defined objective.

The current state of the developed framework includes conservation and process equations for the involved components and substances. This permits first optimisation results and constitutes the basis for future design questions of the process such as component dimensioning, topological choices and cost-optimal operation.

To this end, a modularised framework representing the reduction process is implemented using PySCIPOpt [18] relying on the non-commercial solver SCIP [19] for mixed integer nonlinear programming.

First results include the optimisation of the energetic system efficiency η_sys for the iron oxide reduction based on the flash reactor process. The process is modelled via system variables ω that describe its topology and functionality. The aim of the optimisation is to maximize the energetic system efficiency $\eta_\mathrm{sys}(\omega)$ with system variables ω in the set of feasible solutions Ω determined by the process equations of the subprocesses and additional boundary conditions:

$$\begin{aligned} \max \quad & \eta_\mathrm{sys}(\omega) \\ \text{s.t.} \quad & \omega \in \Omega. \end{aligned} \tag{10}$$

The decision variables for the optimisation include the previously introduced hydrogen equivalence ratio λ_{H_2} as well as the reactor temperature T_R.

3. Storage of Renewable Energy within Iron

As briefly described in Section 2.1., the reduction of iron oxides to iron can be carried out using hydrogen. This enables the reduction process to be linked to the hydrogen obtained from water splitting using RE and thus stores the RE in iron. While the reduction of iron oxides today relies heavily on the use of fossil reducing agents, the steel/iron industry is developing innovative processes that are more energy efficient and environmentally friendly. In the following, two processes that can be operated with green hydrogen are presented and evaluated.

3.1. Shaft Furnace direct Reduction of Iron Oxides

The reduction of iron using a shaft furnace reactor is an established technology and is operated in numerous plants around the world, mainly in the form of the commercially available MIDREX® process [20]. In the shaft furnace, iron oxides pellets (5 mm to 15 mm diameter) are fed into the upper end of the reactor and brought into contact with the reducing agent, which is introduced at the lower end of the reactor in a countercurrent flow. Nowadays, mixtures of CO and H_2 are used as reducing agent. However, the use of 100 % H_2 is being investigated and expected to reach emission targets for the steel industry. Since the required particle size for the combustion of iron is estimated to be in the range of 20 µm, additional process steps besides the thermochemical reduction with green hydrogen are necessary to meet the differing particle size requirements. The process considered is shown in Fig. 3.

The starting point are the fine iron oxide particles from the previous oxidation. Since the shaft furnace requires relatively large pellets, the fine iron oxide particles must be agglomerated, which can be done by pelletisation. During pelletisation, the particles are mixed with water and a binder, and are formed into so called ”green pellets”. In the following, these green pellets are dried and indurated at high temperatures to withstand the stresses in the shaft furnace. In the process under consideration, only the induration is covered: First, the green pellets are heated with hot air to the required temperature of 1473 K to 1573 K [21] and subsequently cooled. The heat for cooling the pellets is recovered to preheat the air. Afterwards the pellets are fed to the shaft furnace. The bottom product of the shaft furnace are the reduced iron pellets, which are transported directly to an electric arc furnace, where the iron is melted and downstream processed. The top gas of the shaft furnace (heavy in H_2O) is used to preheat the hydrogen stream fed to the furnace. A large part of the water within the cooled top gas of the shaft furnace is separated by a downstream condenser. Due to the required fine-grained powder, the reduced pellets have to be further processed. Fine iron particles are usually produced by water atomisation [22] in which the iron is melted and subsequently atomised with a stream of water to produce fine particles.

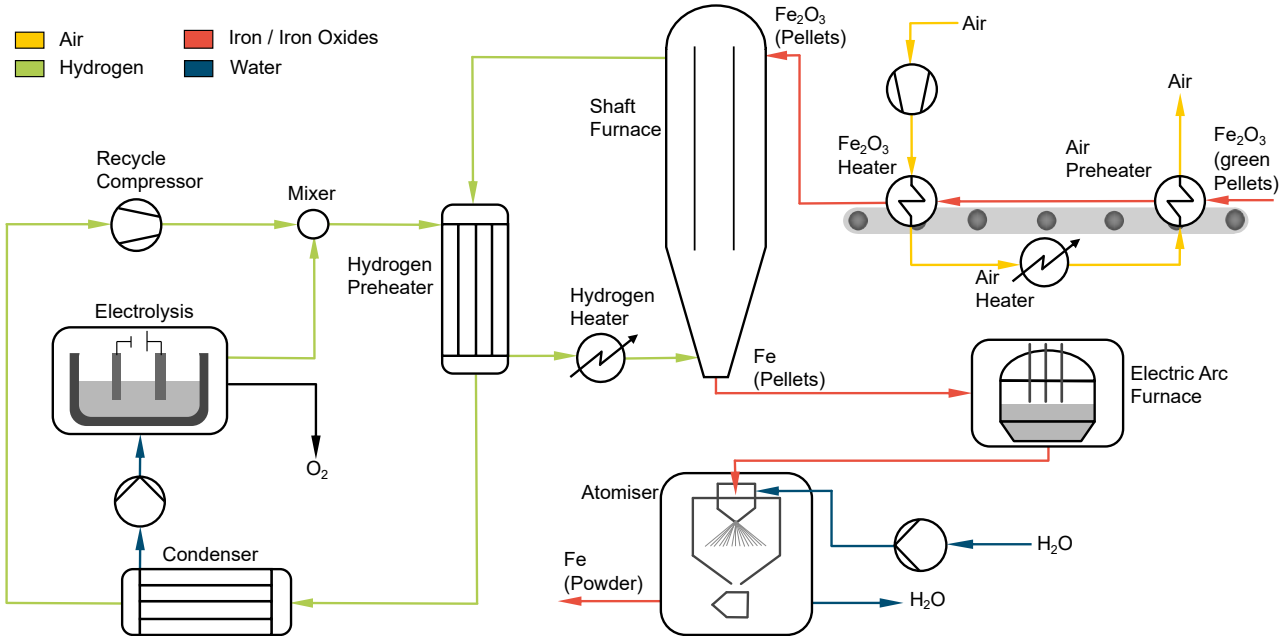

Figure 3: Flow sheet of the shaft furnace reduction process with the required periphery.

3.1.1. Assumptions and Parameterisation

The system efficiency of the water electrolysis $\eta_{\text{electrolysis}}$ is set to 84 % based on the HHV of hydrogen (71 % based on LHV), which is in line with predicted efficiencies for 2030 [23]. The efficiency of the turbo machinery is set to 80 % including the efficiencies of electric motors. Relative heat losses in all heat exchangers Φ_{HEX} are set to 5 % of the transferred heat $\dot{Q}_{\text{tran}}$ (i.e., $\Phi_{\text{HEX}} = \dot{Q}_{\text{loss}}/\dot{Q}_{\text{tran}}$). The approach temperature ΔT_{HEX} is set to 30 K for all heat exchangers, which is further increased due to the previously introduced heat losses. For the pellet temperature at the end of the induration a temperature of 473 K is assumed and the outlet temperature of the condenser is set to 308 K. The resulting particle size distribution of the water atomisation depends on a variety of process parameters (feed temperature of the melt, water pressure and the design and arrangement of the nozzles)[22]. The water pressure is set to 20 MPa, the temperature of the molten iron is set to 1873 K (about 60 K above the melting temperature of iron), while the water mass flow is selected so that the temperature of

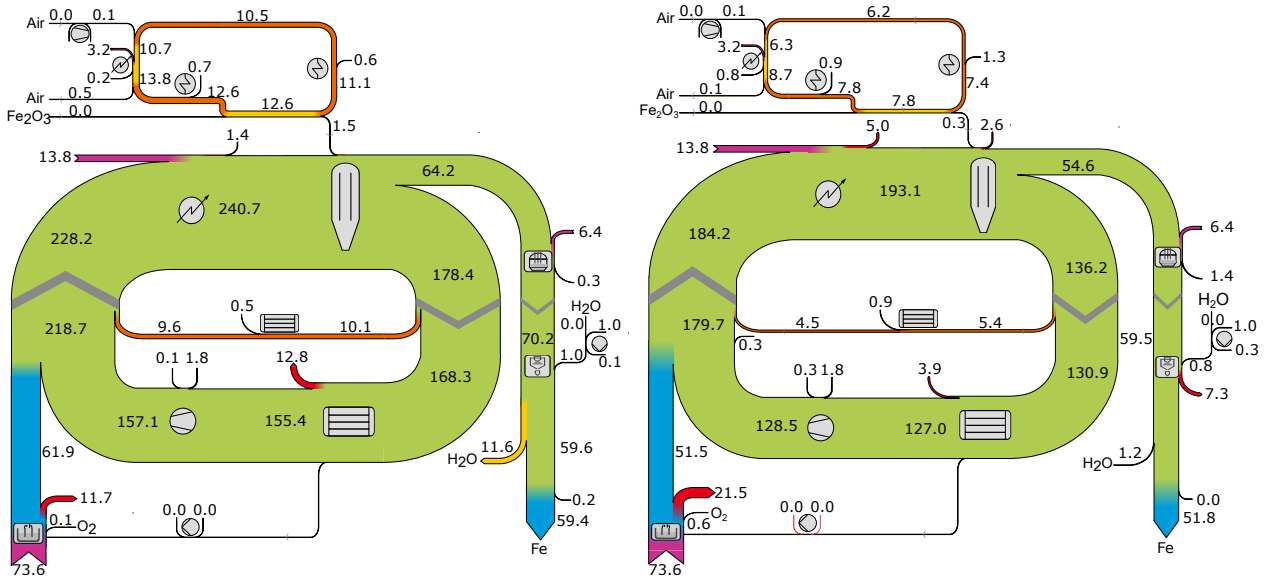

(a) Energy Sankey diagram

(b) Exergy Sankey diagram

Figure 4: Sankey diagrams for the shaft furnace reduction process. Numerical values refer to the relative energy/exergy content in relation to the total energy/exergy provided. ■ energy/exergy transfer associated with (electrical) work, ■ energy/exergy transfer associated with heat, ■ total energy/exergy associated to a stream of matter, ■ physical energy/exergy associated to a stream of matter, ■ chemical energy/exergy associated to a stream of matter, ■ energy loss or exergy destruction.

the mixture at the end of the atomiser is slightly below the evaporation temperature of water. Pressure drops in all heat exchangers are set to 5 kPa and to 100 kPa for the shaft furnace. The heat losses for the shaft furnace and the hydrogen heater are attributed to the hydrogen preheater and account for 10 % of the heat provided at the hydrogen preheater. The adiabatic shaft furnace is modelled via two successive equilibrium reactors, with the temperature of the lower reactor T_R equal to 1173 K (equilibrium reactor one), a temperature difference of 150 K to the second reaction zone (equilibrium reactor two) and a subsequent preheating zone modelled as a heat exchanger. Heat losses of the electric arc furnace are estimated to be 5 % of the provided heat as well. All required process heat is provided by electrical heaters and the hydrogen equivalence ratio at the reactor inlet is set to $\lambda_{H_2} = 3.5$. The system pressure p_{sys} after mixing the recycled with the fresh H_2 stream is set to 200 kPa.

3.1.2. Results and Discussion

With the aforementioned parameterisation, an energetic efficiency of $\eta_{sys} = 59.4\,\%$ is determined. The corresponding energy Sankey diagram is shown in Fig. 4a, in which the numerical values refer to the relative energy content in relation to the total energy supplied to the system (e.g., a numerical value of 50 corresponds to 50 % of the total energy supplied to the system). The largest energy losses are caused by the heat dissipated at the condenser, the physical energy associated to the residual water of the atomiser and the electrolysis.

The exergetic analysis (Fig. 4b) shows that the highest exergetic losses can be associated to the water electrolysis, the unavoidable mixing of water and molten iron during water atomisation and the hydrogen heater. An exergetic efficiency of $\epsilon_{sys} = 51.8\,\%$ is determined. The process efficiency suffers from the required pelletisation and the water atomisation, which can be seen as thermodynamic dissipative subprocesses due to the additional energy requirements without thermodynamic gain (minor gain for the agglomeration of the particles, since the warm particles are directly fed to the reactor).

In Section 3.1.1. a number of parameters for the process are estimated. Subsequently, the effects of these parameters are quantified with one-dimensional sensitivity analyses in relation to the energetic system efficiency (see Fig. 5). For all parameters assessed, the iron oxide is completely reduced to iron. The greatest influence on the energetic system efficiency, similar to other hydrogen-based fuels, has the efficiency of the water electrolysis. Besides, heat recovery (reflected by heat losses and the approach temperatures) also has great influence on the efficiency of the process. The difference between neglecting heat losses and doubling them is four percentage points and for varying the approach temperature for the heat exchangers it is roughly one percentage point. Variations in the hydrogen equivalence ratio lead to a change in the power requirement for the compressor and the heat requirement in the hydrogen preheater (three percentage points in the considered interval). This holds also, with a smaller impact, for the variation of the system pressure. The higher the system pressure, the more water condenses and consequently the mass flow of the recycle stream is lower,

which reduces the power requirement of the turbo machinery and the hydrogen heater. Interestingly, the reactor temperature has a rather low impact on the efficiency (less than one percentage point). The reason is that the energy demand of the subsequent electric arc furnace is decreasing with increasing reactor temperature. The combination of the individual optimal values (reactor temperature and electrolysis efficiency kept according to the reference values) leads to energetic efficiencies above 63 %.

It is emphasised that all calculations are based on chemical equilibrium calculations for the reduction of iron oxides. Despite the long residence times in the shaft furnace, reaction kinetics and transport phenomena can be limiting, which is not taken into account in the equilibrium model. In addition, all required process heat is provided by electric heaters. However, due to the high temperatures, the electric heaters will most likely be replaced by burners using carbon neutral fuels (e.g., H_2), leading to further inefficiencies. During water atomisation, oxidation of the freshly reduced particles occurs to some extent, which is also not covered. This can be countered with inert gas atomisation, which, however, has high energy requirements for the gas compression and the production of the inert gas (i.e., air separation) itself, if the inert components cannot be fully recycled. Nevertheless, the shaft furnace direct reduction with hydrogen relies on existing processes that are already utilised on an industrial scale, and thus could also be used for the energy-iron cycle in the near future.

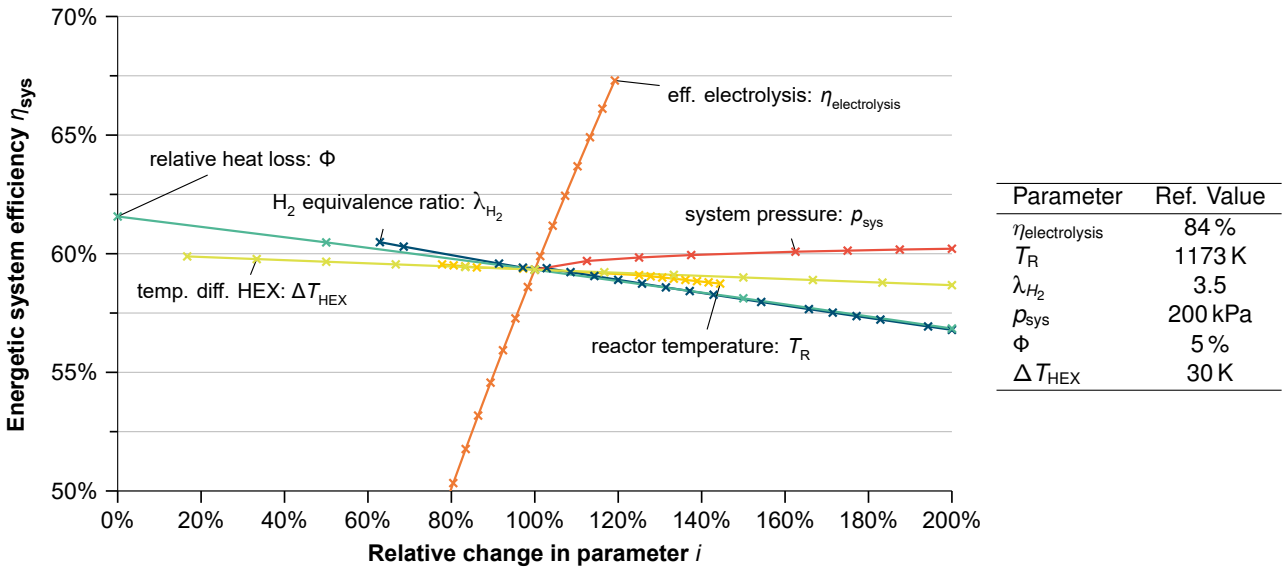

Parameter	Ref. Value
$\eta_{electrolysis}$	84 %
T_R	1173 K
λ_{H_2}	3.5
p_{sys}	200 kPa
Φ	5 %
ΔT_{HEX}	30 K

Figure 5: One-dimensional analysis of selected parameters on the energetic system efficiency for the shaft furnace process.

3.2. Flash Reactor direct Reduction of Iron Oxides

A novel flash reactor technology is currently developed at the University of Utah [24–26]. With this technology, fine iron oxide particles can be reduced using a suitable reducing gas (e.g., hydrogen, natural gas or a combination thereof). Unlike the shaft furnace process, the flash reactor technology is able to utilise the fine iron oxide particles directly and without upstream treatment, eliminating the need for the agglomeration (pelletisation) and subsequent water atomisation, making it the ideal regeneration process for the energy-iron cycle. At the University of Utah such a system is currently operated in the form of a mini pilot reactor [25]. Using the gained expertise, a model-based design of an industrial-scale flash iron-making process was carried out, which shows promising results [26]. The investigated process is shown in Fig. 6.

The starting point is the iron oxide powder from the preceding oxidation. The particles are fed to a bulk heat exchanger to preheat them before they are fed into the flash reactor in combination with preheated hydrogen leading to a co-current flow of both reactants. The heterogeneous gas-solid mixture is then fed into a cyclone to separate the solids from the gaseous components. While the heat of the solid iron particles is recovered using air as a secondary fluid in bulk heat exchangers, the heat of the gaseous products (H_2 and H_2O) is used to preheat the hydrogen fed to the reactor. Finally, most of the water is separated by a condenser before the residual hydrogen stream is recycled through a compressor.

3.2.1. Assumptions and Parameterisation

The parameterisation of the flash reactor reduction process is analogous to the parameterisation of the shaft furnace reduction in Section 3.1.1. In deviation to the shaft reduction process, the pressure losses of the reactor and cyclone are set to 5 kPa. The system pressure after mixing the recycled H_2 stream with the fresh

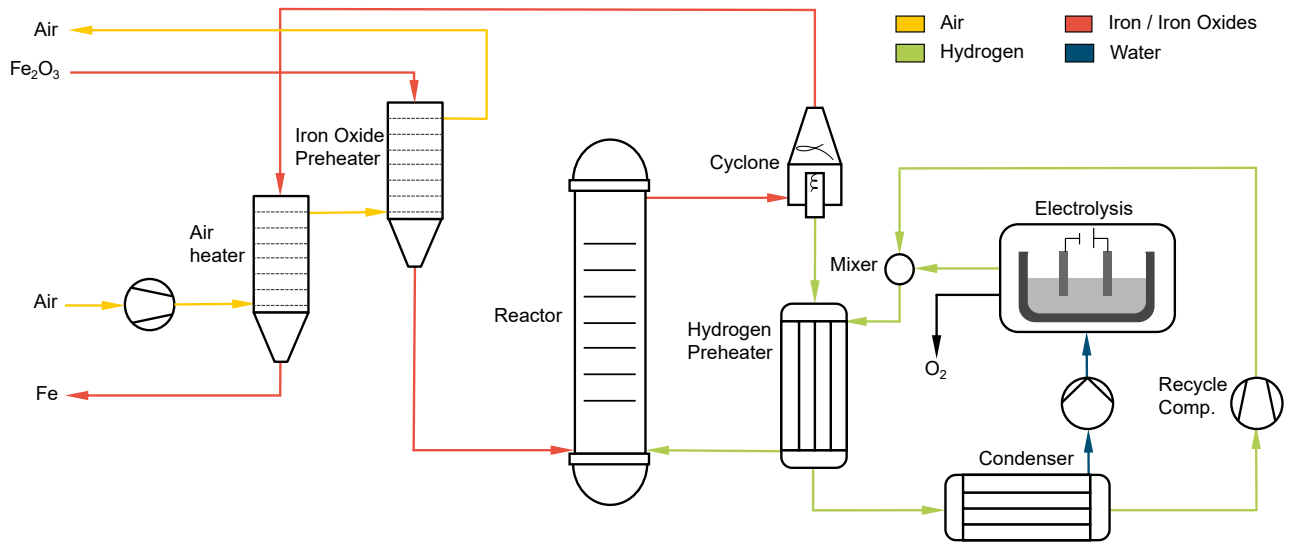

Figure 6: Flow sheet of the flash reduction process.

H_2 stream is set to 100 kPa instead of 200 kPa, since the pressure losses in the reactor are significantly lower.

3.2.2. Results and Discussion

With the aforementioned parameterisation an energetic efficiency of η_{sys} = 68.5 % is determined. The corresponding energy Sankey diagram is shown in Fig. 7a. The largest energy losses are caused by the heat dissipated in the condenser, followed by the energy losses related to the electrolysis and the heat losses of the heat exchangers. The exergetic analysis (see Fig. 7b) shows that the highest exergetic destructions are associated to the water splitting, the flash reactor and the condensers. An exergetic efficiency of ϵ_{sys} = 59.9 % is obtained.

As mentioned in Section 2.4., the flash reactor process was modelled in a developed process simulation framework for process modelling and direct optimisation. The energetic efficiency with the above described parametrisation is η_{sys} = 69.2 %, which corresponds to a deviation of 0.7 percentage points from the value obtained with the use of commercial software. The deviation is assumed to be caused by modelling simplifications for the substance data.

In the same manner as for the shaft furnace process, the effects of the assumptions from Section 3.2.1. are again quantified with a one-dimensional sensitivity analyses with respect to the energetic system efficiency (see Fig. 8). For all parameters assessed, the iron oxide is completely reduced to iron. Similar to the shaft furnace reduction process, the efficiency of the water electrolysis has the greatest influence on the energetic system efficiency. Analogously, heat recovery has a great influence on the efficiency of the process. The difference between neglecting heat losses and doubling them is 2.5 percentage points, which is slightly lower compared to the shaft furnace reduction, since less units with corresponding heat loss are required. The impact of the approach temperature for the heat exchangers is approximately in the same order (one percentage point). Variations in the hydrogen equivalence ratio lead to a change in the power requirement for the compressor and the heat requirements for the flash reactor (2.5 % in the considered interval). This holds also, with a smaller impact, for the variation of the system pressure. The higher the system pressure, the more water condenses and consequently the mass flow of the recycle stream is lower, which reduces the power requirements of the turbo machinery and the reactor. In deviation to the shaft furnace reduction, the reactor temperature has a higher impact on the efficiency (2.5 percentage points compared to roughly one percentage point). Since there is no subsequent process requiring high temperatures (i.e., electric arc furnace) increasing reactor temperatures despite the bulk solid heat exchangers lead to increasing losses. The combination of the individual optimal values (reactor temperature and electrolysis efficiency kept according to the reference values) leads to an energetic efficiencies of approximately 71 %.

It is again emphasised that all calculations are based on chemical equilibrium calculations for the reduction of iron oxides with hydrogen. While this might be acceptable for the shaft furnace reduction due to the long residence times (order of minutes), this assumptions may lead to significant errors, due to the short residence (order of seconds) within the flash reactor. In the same manner as for the shaft furnace, the required process heat is provided by electric heaters. However, the high temperatures are unlikely to be achieved with electric heaters and will most likely be replaced by burning carbon neutral fuels (e.g., H_2), leading to further inefficiencies. Furthermore, the use of bulk solid heat exchangers might not be feasible or useful due to technological limitations (high temperatures) or sticking of particles within the exchangers. If the heat released from the hot

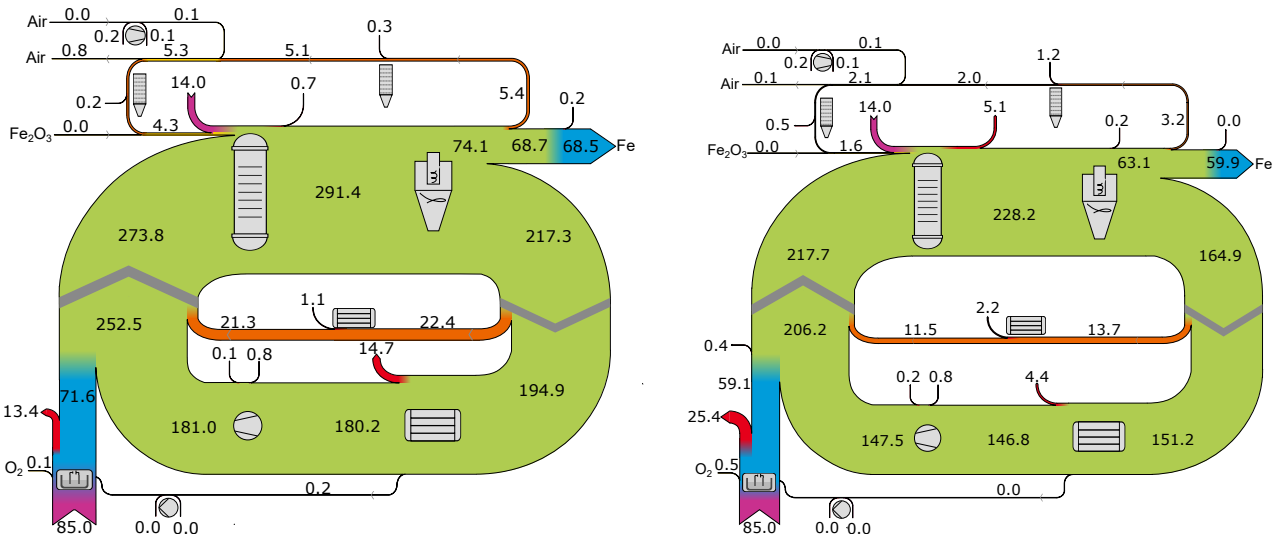

(a) Energy Sankey diagram

(b) Exergy Sankey diagram

Figure 7: Sankey diagrams for the flash reactor reduction process. Numerical values refer to the relative energy/exergy content in relation to the total energy/exergy provided. ■ energy/exergy transfer associated with (electrical) work, ■ energy/exergy transfer associated with heat, ■ total energy/exergy associated to a stream of matter, ■ physical energy/exergy associated to a stream of matter, ■ chemical energy/exergy associated to a stream of matter, ■ energy loss or exergy destruction.

iron particles cannot be recovered, the system efficiency for the given system is reduced by approximately three percentage points to 65.7 %.

The mathematical optimisation of the system with the used parameters of the sensitivity analysis as decision variables leads to η_{sys} = 73.1 %. Additional to the obvious adaptions regarding heat losses (Φ = 0) and approach temperature $\Delta T_{HEX} \approx 0$, the optimisation adjusts the reactor temperature to T_R = 843 K (lower bound) and the hydrogen equivalence ratio to λ_{H_2} = 5.4. While the results can be regarded as correct within the model assumptions (i.e., thermodynamically controlled reactor model), the results most likely cannot be transferred to real applications, since the reaction speed at these low temperatures would require residence times which are multiple magnitudes too high. However, the results reflect the application potential for optimisation, which will unfold its superiority with increasing model accuracy (i.e., kinetically controlled reactor model) and conflicting decision criteria (e.g., capital and operation costs).

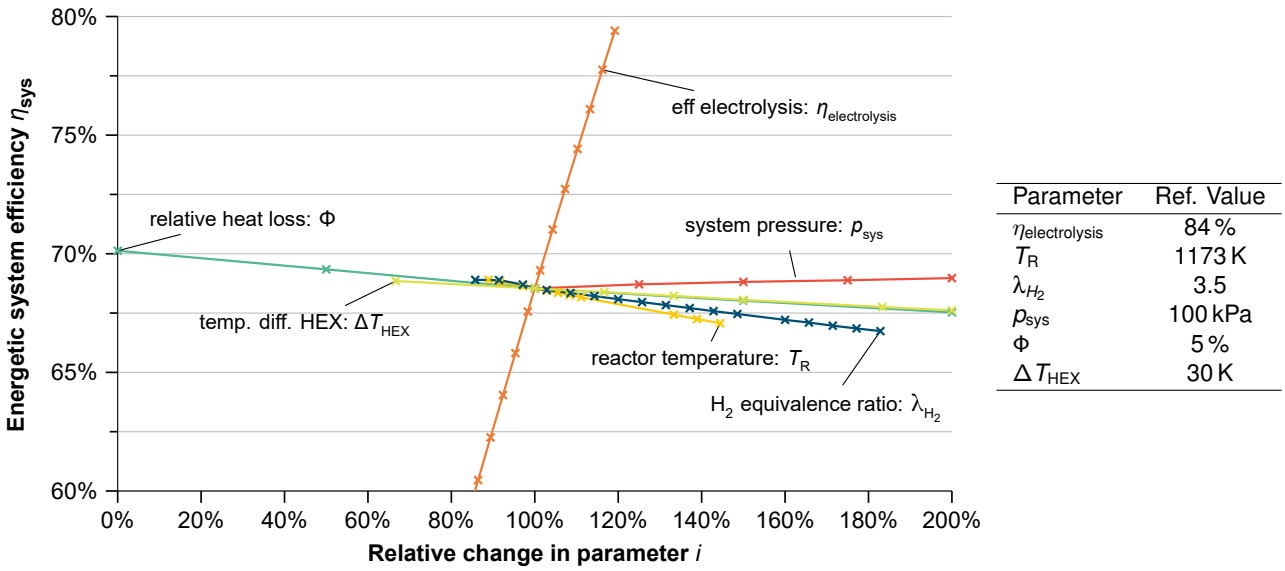

Parameter	Ref. Value
$\eta_{electrolysis}$	84 %
T_R	1173 K
λ_{H_2}	3.5
p_{sys}	100 kPa
Φ	5 %
ΔT_{HEX}	30 K

Figure 8: One-dimensional analysis of selected parameters on the energetic system efficiency for the flash reduction process.

4. Conclusion and Outlook

Metal fuels and especially iron as recyclable energy carrier can enable the successful transition to carbon-neutral energy systems by addressing the temporal and geographic mismatch between renewable energy supply and demand. A meaningful evaluation of the energy-iron cycle requires a holistic system approach which has to consider all subprocesses and promising variants, diverse evaluation criteria (e.g., efficiencies, costs, environmental impact), and various deployment scenarios. With the overall goal of a holistic system analysis, this study provides quantitative and qualitative information on the thermodynamic performance of two potential regeneration processes for the iron oxides utilising a shaft furnace or a flash reactor.

The shaft furnace direct reduction of iron oxides is a process which is today operated on industrial scale using synthesis gas but can be operated using 100 % hydrogen. For a defined reference case, including water electrolysis, energetic and exergetic efficiencies of η_{sys} = 59.4 % and ϵ_{sys} = 51.8 %, respectively, are determined using commercial process simulation software. A one-dimensional sensitivity analysis shows that an energetic efficiency of η_{sys} = 63 % is theoretically achievable, whereby the highest impact besides the electrolysis efficiency is shown by means of heat recovery (heat loss and approach temperatures minimised). While the shaft furnace direct reduction itself is highly efficient, the requirements for the particle sizes differ compared to the anticipated release process (i.e., oxidation of fine-grained iron powder), which makes additional process steps (pelletisation and water atomisation) necessary, decreasing the overall system efficiency. In contrast to the shaft furnace direct reduction, a flash reactor can directly use the fine particles required for oxidation, leading to energetic and exergetic efficiencies of η_{sys} = 68.5 % and ϵ_{sys} = 59.9 %, respectively, with an analogous parameterisation compared to the shaft furnace process. Here, the combination of optimal values based on the sensitivity analysis leads to η_{sys} = 71.0 %. Parallel to the use of commercial process simulation software, a modelling environment with direct access to mathematical optimisation techniques has been developed and showcased for the flash reduction process and indicates good agreement. The application of the optimisation algorithms leads to an efficiency of η_{sys} = 73.1 %.

Both modelling approaches utilise chemical equilibrium calculations (thermodynamically controlled reaction) for the reduction reaction of iron oxides with hydrogen. While this might be acceptable for the shaft furnace direct reduction due to long residence times, this might lead to significant deviations due to short residence times within the flash reactor (kinetically controlled reaction). Nevertheless, the results suggest that storage efficiencies of 60 % to 70 % might be achievable using state of the art and perspective technologies, respectively.

Next steps are the inclusion of adequate kinetic information for the considered processes using available models from the literature. Furthermore, the models will be expanded from purely thermodynamic models to thermoeconomic models to allow the economic evaluation and optimisation. Due to the increasing complexity, the developed modelling environment with direct access to mathematical optimisation algorithms will unfold its potential.

Acknowledgments

The authors would like to thank the speakers of the collaborative project Clean Circles Andreas Dreizler and Christian Hasse for their conceptual work on the energy-iron cycle, which is presented in the introduction of this paper. We would also like to thank Johannes Janicka, who performed initial simulations on the reduction process of iron oxides with hydrogen, from which this work has benefited. Furthermore, the funding of the cluster project Clean Circles by the Hessian Ministry of Higher Education, Research, Science and the Arts is gratefully acknowledged.

Nomenclature

- e specific exergy, $\mathrm{J\,kg^{-1}}$
- $\dot{E}$ time rate of exergy transfer, $\mathrm{J\,s^{-1}}$
- h specific enthalpy, $\mathrm{J\,kg^{-1}}$
- $\dot{m}$ mass flow rate, $\mathrm{kg\,s^{-1}}$
- P time rate of energy transfer associated with work, $\mathrm{J\,s^{-1}}$
- $\dot{Q}$ time rate of energy transfer associated with heat, $\mathrm{J\,s^{-1}}$
- R specific gas constant, $\mathrm{J\,kg^{-1}\,K^{-1}}$
- s specific entropy, $\mathrm{J\,kg^{-1}\,K^{-1}}$

T	temperature, K
x	mass fraction
y	mole fraction

Greek symbols

Δ	difference
ϵ	exergetic efficiency
η	energetic efficiency
λ	hydrogen equivalence ratio
ω	set of system variables
Φ	relative heat loss
Ω	set of feasible solutions

Subscripts and superscripts

ch	chemical
D	destruction
L	loss
ph	physical
Q	heat
r	reaction
R	reactor
sys	system
tot	total
tran	transferred
0	standard, reference

References

[1] Climate Watch. World Greenhouse Gas Emissions in 2018 by Sector, End Use and Gases (static). URL: https://www.climatewatchdata.org/key-visualizations?visualization=4 (visited on Mar. 6, 2022).

[2] German Environment Agency. Renewable energy share in gross final energy consumption and gross electricity consumption. URL: https://www.umweltbundesamt.de/en/data/environmental-indicators/indicator-renewable-energy#at-a-glance (visited on Mar. 10, 2022).

[3] AG Energiebilanzen e.V. Energy Flow Chart for the Federal Republic of Germany in 2020. URL: https://ag-energiebilanzen.de/wp-content/uploads/2021/09/ageb_energieflussbild-kurz_engl-2022-pj_20210923.pdf (visited on Mar. 6, 2022).

[4] Ohlig K. and Decker L. The latest developments and outlook for hydrogen liquefaction technology. In: AIP Conference Proceedings. AIP Publishing LLC, 2014, pp. 1311–1317. DOI: 10.1063/1.4860858.

[5] The International Renewable Energy Agency. Green hydrogen cost reduction: Scaling up electrolysers to meet the 1.5C climate goal. 2020. URL: https://irena.org/-/media/Files/IRENA/Agency/Publication/2020/Dec/IRENA_Green_hydrogen_cost_2020.pdf (visited on June 14, 2021).

[6] Bergthorson J. M. Recyclable metal fuels for clean and compact zero-carbon power. In: *Progress in Energy and Combustion Science* 68 (2018), pp. 169–196. DOI: 10.1016/j.pecs.2018.05.001.

[7] Bergthorson J. M. et al. Direct combustion of recyclable metal fuels for zero-carbon heat and power. In: *Applied Energy* 160 (2015), pp. 368–382. ISSN: 03062619. DOI: 10.1016/j.apenergy.2015.09.037.

[8] Dirven L., Deen N. G., and Golombok M. Dense energy carrier assessment of four combustible metal powders. In: *Sustainable Energy Technologies and Assessments* 30 (2018), pp. 52–58. ISSN: 22131388. DOI: 10.1016/j.seta.2018.09.003.

[9] Yavor Y. et al. Comparative reactivity of industrial metal powders with water for hydrogen production. In: *International Journal of Hydrogen Energy* 40.2 (2015), pp. 1026–1036. ISSN: 03603199. DOI: 10.1016/j.ijhydene.2014.11.075.

[10] Barelli L. et al. Reactive Metals as Energy Storage and Carrier Media: Use of Aluminum for Power Generation in Fuel Cell–Based Power Plants. In: *Energy Technology* 8.9 (2020), p. 2000233. ISSN: 2194-4288. DOI: 10.1002/ente.202000233.

[11] A. Dreizler and C. Hasse – Speakers of Clean Circles, Technical University Darmstadt, University of Applied Sciences Darmstadt. Overview Clean Circles. URL: https://www.tu-darmstadt.de/clean-circles/about_cc/research_summary_cc/index.en.jsp (visited on Mar. 9, 2022).

[12] Team Solid – Eindhoven University of Technology. Projects Overview. URL: https://teamsolid.org/algemene-content-pagina-voorbeeld/projects/ (visited on Mar. 1, 2022).

[13] Spreitzer D. and Schenk J. Iron Ore Reduction by Hydrogen Using a Laboratory Scale Fluidized Bed Reactor: Kinetic Investigation—Experimental Setup and Method for Determination. In: *Metallurgical and Materials Transactions B* 50.5 (2019), pp. 2471–2484. ISSN: 1073-5615. DOI: 10.1007/s11663-019-01650-9.

[14] McBride B. J. and Gordon Stanford. Computer Program for Calculation of Complex Chemical Equilibrium. Ed. by NASA. 1996. URL: https://ntrs.nasa.gov/citations/19950013764 (visited on Mar. 4, 2022).

[15] Bejan A., Tsatsaronis G., and Moran M. J. Thermal design and optimization. New York and Chichester: John Wiley, 1996. ISBN: 0471584673.

[16] STEAG Energy Services GmbH. EBSILON Professional. URL: https://www.ebsilon.com/en/ (visited on Mar. 3, 2022).

[17] McBride B. J., Zehe M. J., and Gordon S. NASA Glenn Coefficients for Calculating Thermodynamic Properties of Individual Species. 2002. URL: https://ntrs.nasa.gov/citations/20020085330 (visited on Feb. 22, 2022).

[18] Maher S. et al. PySCIPOpt: Mathematical Programming in Python with the SCIP Optimization Suite. In: *Mathematical Software ICMS 2016*. Springer International Publishing, 2016, pp. 301–307. DOI: 10.1007/978-3-319-42432-3{\textunderscore}37.

[19] Bestuzheva K. et al. The SCIP Optimization Suite 8.0: Technical Report. 2021. URL: http://www.optimization-online.org/DB_HTML/2021/12/8728.html.

[20] Midrex Technologies, Inc. World Direct Reduction Statistics. 2020. URL: https://www.midrex.com/wp-content/uploads/Midrex-STATSbookprint-2020.Final_.pdf (visited on Feb. 21, 2022).

[21] Moraes S. L. de, Lima J. R. B. de, and Ribeiro T. R. Iron Ore Pelletizing Process: An Overview. In: *Iron Ores and Iron Oxide Materials*. Ed. by V. Shatokha. InTech, 2018. ISBN: 978-1-78923-320-9. DOI: 10.5772/intechopen.73164.

[22] Dossett J. L. and Totten G. E. ASM Handbook: Powder Metal Technologies and Applications. Vol. 7. Materials Park, Ohio: ASM International, 1998. ISBN: 9780871703873.

[23] International Energy Agency - IEA. The Future of Hydrogen. 2019. URL: https://iea.blob.core.windows.net/assets/9e3a3493-b9a6-4b7d-b499-7ca48e357561/The_Future_of_Hydrogen.pdf (visited on June 14, 2021).

[24] Chen F. et al. Hydrogen Reduction Kinetics of Hematite Concentrate Particles Relevant to a Novel Flash Ironmaking Process. In: *Metallurgical and Materials Transactions B* 46.3 (2015), pp. 1133–1145. ISSN: 1073-5615. DOI: 10.1007/s11663-015-0332-z.

[25] Sohn H. Y. Energy Consumption and CO2 Emissions in Ironmaking and Development of a Novel Flash Technology. In: *Metals* 10.1 (2020), p. 54. DOI: 10.3390/met10010054.

[26] Sohn H. Y., Fan D.-Q., and Abdelghany A. Design of Novel Flash Ironmaking Reactors for Greatly Reduced Energy Consumption and CO2 Emissions. In: *Metals* 11.2 (2021), p. 332. DOI: 10.3390/met11020332.

Urheberrechtsschutz

Dieses Objekt ist durch das Urheberrecht und/oder verwandte Schutzrechte geschützt. Sie sind berechtigt, das Objekt in jeder Form zu nutzen, die das Urheberrechtsgesetz und/oder einschlägige verwandte Schutzrechte gestatten. Für weitere Nutzungsarten benötigen Sie die Zustimmung der/des Rechteinhaber/s.

Hinweise:

- Möglicherweise benötigen Sie zusätzliche Erlaubnisse für die beabsichtigte Nutzung. Zum Beispiel weil andere Rechte, wie Veröffentlichungsrechte, Persönlichkeits- oder Urheberpersönlichkeitsrechte den erlaubten Nutzungsumfang einschränken.
- Möglicherweise finden Sie zusätzliche Informationen zum Urheberrechtsschutz des Objekts auf der Website der Institution, die das Objekt verfügbar gemacht hat.
- Soweit nicht ausdrücklich an anderer Stelle ausgewiesen, gibt die Institution, die das Objekt zugänglich gemacht hat, keine Zusicherungen in Bezug auf dieses und übernimmt keine Garantie für die Richtigkeit des gewählten Rechtehinweises. Sie sind für die eigene Nutzung selbst verantwortlich.